

# MEASUREMENT OF FIBRE FRACTURE TOUGHNESS USING AN ALTERNATIVE SPECIMEN GEOMETRY

**Mauricio V. Donadon, Brian G. Falzon, Lorenzo Iannucci, John M. Hodgkinson**  
Imperial College London

**Keywords:** *Composites, fracture mechanics, fracture toughness, finite elements*

## **Abstract**

*This paper presents an experimental and numerical study focused on the tensile fibre fracture toughness characterisation of hybrid plain weave composite laminates using non-standardized Overheight Compact Tension (OCT) specimens. The position as well as the strain field ahead of the crack tip in the specimens was determined using a digital speckle photogrammetry system. The limitation on the applicability of standard data reduction schemes for the determination of the intralaminar fibre fracture toughness of composites is presented and discussed. A methodology based on the numerical evaluation of the strain energy release rate using the J-integral method is proposed to derive new geometric correction functions for the determination of stress intensity factor for alternative composite specimen geometries. A comparison between different methods currently available to compute the intralaminar fracture toughness in composites is also presented and discussed. Good agreement between numerical and experimental results using the proposed methodology was obtained.*

## **1 Introduction**

The measurement of the intralaminar fracture toughness in composites requires a pre-cracked specimen and in most cases, is based on Linear Elastic Fracture Mechanics (LEFM). Different specimen and crack geometries are currently available in the literature to characterise the intralaminar fracture behaviour of composites [1 - 3], but no standard exists.

Jose et al. [4] investigated the mode I intralaminar toughness of carbon/epoxy cross-ply laminates using overheight compact tension specimens. The experimental results were compared with finite element simulations using a modified crack-closure integral method and a methodology for calculating the stress intensity factor associated

with matrix cracking and fibre fracture was presented. Based on the work by Jose et al. [4], Pinho et al. [5] investigated the intralaminar toughness associated with fibre breakage in tension and fibre kinking in compression in unidirectional pre-preg composites using Compact Tension (CT) and Compact Compression (CC) specimens. A very consistent resistance curve (R-Curve) containing initiation and propagation values was obtained in tension, with a marked increase in the toughness values in compression due to fibre compression kinking. The authors attribute the increase in the toughness in compression to the contact in the crushed area. In fact, the contact is a problem even in tension, if the specimen is subjected to cyclic loading-unloading cycles, due to debris effects which impede the total closure of the crack, giving rise to permanent displacements [6]. Kostopoulos and co-workers [6] proposed a modified compliance method to handle problems in which permanent displacements are an important issue. The method is based on the Non-Linear Fracture Mechanics (NLFM) approach and the resultant nonlinear fracture toughness is composed of elastic and non-elastic terms due to the presence of irreversible deformations. The method uses an effective crack length based on a semi-empirical equation.

The specimen selection depends on the material system under investigation and results for the initiation and propagation values of fracture toughness are usually sought. It is also worth mentioning that most of the specimens were originally designed for isotropic materials. The poor performance of composites in shear and compression loading, compared to tensile loading in the fibre direction may lead to failure prior to crack growth. Such restrictions impose limitations on established specimen geometries and alternative specimen designs are needed.

The present work investigates the fibre fracture toughness of composite laminates using a

modified Compact Tension (CT) specimen and builds on the work presented in [7]. The determination of the fibre fracture toughness was initially assessed using the compliance method. Additionally the validity of the standards for evaluating the stress intensity factor was investigated by finite element analysis using the J-integral method. Based on the correlation between numerical and experimental results, a new polynomial geometric function was proposed for computing the stress intensity factor. Implicitly, the new correction function accounts for finite geometry and orthotropic effects.

## 2 Materials and laminates manufacturing

Laminates with a hybrid plain weave fabric [90/0<sub>3</sub>]<sub>2s</sub> lay-up were manufactured using Resin Infusion under Flexible Tooling (RIFT) process. Each ply consisted of an unidirectional fabric supplied by EUROCARBON<sup>®</sup>, composed of T700-12K-50C carbon fibres in the longitudinal direction with a small volume fraction of PPG EC09 34\*2 S150 1383 glass fibres in the transverse direction. The resin system consisted of PRIME 20LV<sup>®</sup> two part epoxy resin system, supplied by SP Systems. All laminates were manufactured using the Resin Infusion under Flexible Tooling (RIFT) process setup outlined in Fig.1. A flat 700mm x 400mm x 4 mm aluminium plate was used as a mould tool. Prior to laying up the fabric, the aluminium plate was covered with a melanex film and one peel ply layer, which aids the removal of the composite plates after cure. The fabrics were covered with a flow distribution medium on the upper and lower surfaces, in order to ensure complete fabric wetting-out.

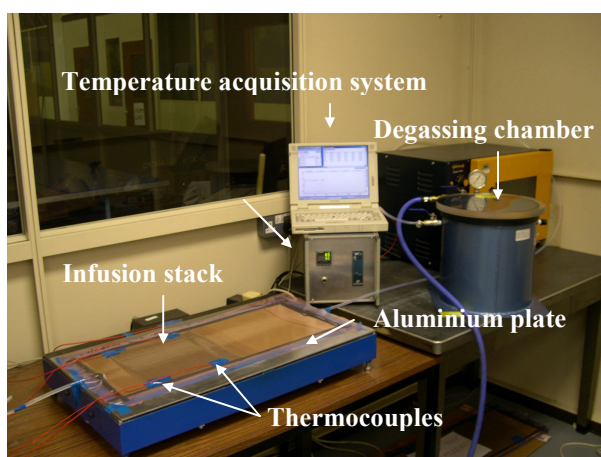


Fig. 1. RIFT setup [8]

The resin flow medium was intentionally cut 30 mm shorter from the end of the preform near the vacuum vent to reduce the resin flow rate within the infusion stack. Subsequently the infusion stack was bagged and placed on the hot platen. Next, vacuum drop tests were carried out by applying full vacuum into the infusion stack and monitoring the pressure using a dial gauge connected to the degassing chamber for 30 minutes. This procedure ensures the vacuum integrity within the RIFT system. Vacuum integrity is possibly the most important manufacturing parameter for the RIFT process. Infusions were carried out at room temperature (25°C), with panels cured for 7 hours at 65°C. The temperature variation of the laminate during the curing stage was measured by attaching thermocouples on the upper surface of the stack. The temperature measurements were taken from five different positions, four of them were placed in each corner of the square plate, while the fifth was in the centre of the plate. The temperatures were recorded by means of a temperature data-logger connected to acquisition software. The point-to-point temperature variation was within +/-5°C. In order to assess the final quality of the laminates, the panels were c-scanned and fibre volume fraction and void content were measured using the acid digestion method. According to c-scan images the laminates were free of any major defect, with a typical value of 53% and 1% for the fibre volume fraction and void content, respectively.

The laminate mechanical properties were measured using standard test methods [9, 10] and are summarised in Table 1.

Table 1. Laminates mechanical properties

Young's modulus in the warp direction, $E_{11}$	100 GPa
Young's modulus in the weft direction, $E_{22}$	8.11 GPa
In-plane shear modulus, $G_{12}$	3.88 GPa
Major in-plane Poisson's ratio, $\nu_{12}$	0.35
Tensile strength in the warp direction, $\sigma'_{f,1}$	2005 MPa
Tensile strength in the weft direction, $\sigma'_{f,2}$	63 MPa
Compressive strength in the warp direction, $\sigma^c_{f,1}$	750 MPa
Compressive strength in the weft direction, $\sigma^c_{f,2}$	170 MPa
In-plane shear strength, $\sigma'_{12}$	60 MPa

### 3 Specimen configuration and crack tip preparation

After manufacturing, specimens were cut from the panels according to dimensions shown in Fig. 2.

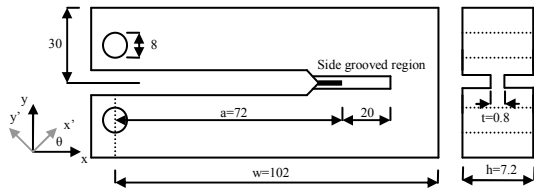


Fig. 2. Modified OCT specimen configuration (dimensions in mm)

The specimens had double the arm length of standard specimens with a side grooved area along the crack growth line. Only two layers orientated at 90° with respect to the global coordinate system were left in the side grooved area with cracking extension normal to the carbon fibre direction. The lay-up and specimen configuration reduce the mean shear stresses and improve the compressive strength of the specimen. It also increases the tensile stresses acting in the cohesive zone avoiding damage in other parts of the specimen prior and during the crack growth stage.

A three step procedure was used to produce a sharp crack tip in the OCT specimens. Firstly a 60 mm length notch was inserted in the specimens using a 3.5mm thick dry diamond saw. Secondly a series of razor saws were used to further increase the crack length by 12 mm; each razor saw employed had progressively increasing number of teeth in the blade, three types were used with each removing 4 mm of material each time. The thickness of the razor saw blade was no more than 0.2mm. Lastly to produce an extreme sharp crack tip a 0.06mm thick razor blade was used lightly to improve the sharpness of the crack tip. A typical micrograph illustrating the quality of the crack tip is shown in Fig. 3.

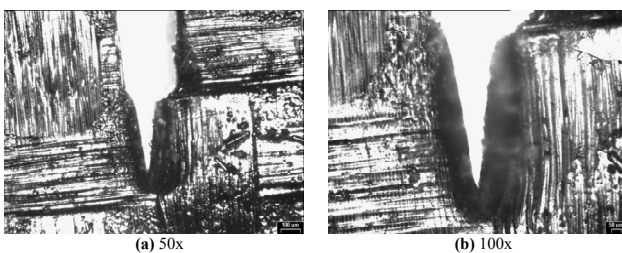


Fig. 3. Crack tip images of the OCT specimens

### 4 Experimental setup

The mechanical tests were carried out using a 10 ton Instron testing machine equipped with a 100kN load cell to measure the load for growing the crack perpendicular to the fibres. The crosshead displacement and load histories were recorded using a data acquisition system. The tests were carried out at a crosshead displacement rate of 1mm/min. A digital speckle photogrammetry system was used in order to visualize the position of the crack tip during the test. Additionally, an extra CCTV camera connected to a monitor was placed normal to the specimen to track the crack growth. By using this extra camera together with a crack event marker, it was possible to determine the load and displacements associated with a specific crack length. The experimental setup for measuring the fibre fracture toughness is shown in Fig.4.



Fig. 4. Experimental setup

### 5 Data reduction scheme

Strictly speaking there are no specific test standards and data reduction schemes to compute the intralaminar fracture toughness for composite materials. Most researchers employ the same data reduction schemes and test standards as the one for isotropic materials; however, their applicability for composites and the reliability of the results are questionable. The expression commonly used for computing the mode-I intralaminar fibre breakage fracture toughness is given by Eq. (1),

$$G_{lc} = K_{lc}^2 (2E_{11}E_{22})^{-0.5} \left( (E_{11}/E_{22})^{0.5} + E_{11}/2G_{12} - \nu_{12} \right)^{0.5} \quad (1)$$

with,

$$K_{lc} = (P/h)(w)^{-0.5} F(a) \quad (2)$$

$$F(a) = 1.98 + 0.36(2a/w) - 2.12(2a/w)^2 + 3.42(2a/w)^3 \quad (3)$$

where  $E_{11}$ ,  $E_{22}$  are the Young's modulus in the longitudinal and transversal directions, respectively and  $G_{12}$  and  $\nu_{12}$  are the in-plane shear modulus and in-plane Poisson's ratio.  $K_{Ic}$  and  $P$  are the stress intensity factor and load for a given crack length  $a$ , respectively and  $F(a)$  is the finite geometry correction function, taken from ASTM E399-90 standard [11].

## 6 Experimental results

A typical load-displacement curve for the modified OCT is shown in Fig. 5.

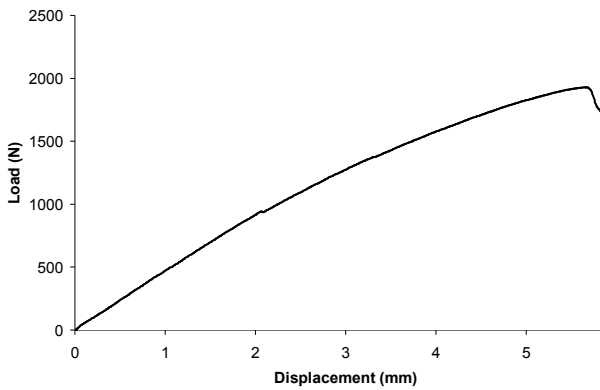


Fig. 5. Load-displacements for the modified OCT specimens

The load-displacement curves exhibited a linear behaviour up to about 900 N without any evidence of crack growth. Non-linearity arises for loads higher than 900 N in which a stable crack growth regime was achieved. The compliance method [12] was applied to calculate the fibre toughness values for the side-grooved specimens. The crack advancement was monitored using the Digital Speckle Photogrammetry (DSP) system and a typical DSP image taken during the test is shown in Fig. 6. The experimental and numerical compliance values versus crack length curves are shown in Fig7.

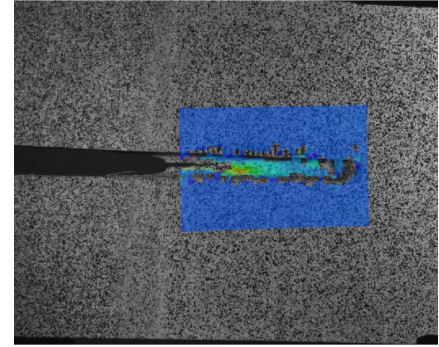


Fig. 6. DSP image of the OCT specimen (region in red indicates the crack tip position)

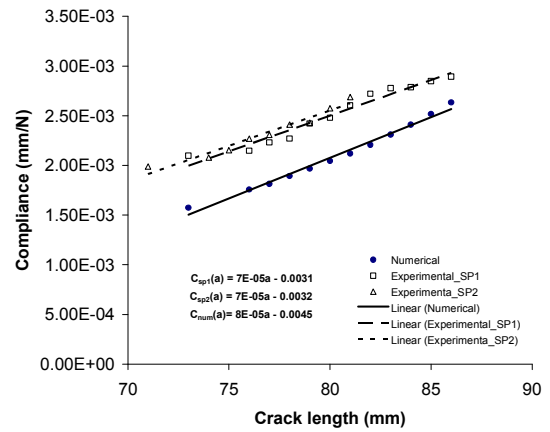


Fig. 7. Load-displacements for the modified OCT specimens

The compliance versus crack length relationship exhibited a fairly linear behaviour within the analysed crack length range. The experimental trend was numerically confirmed and the numerical results correlate reasonably well with experiments. It was observed that the crack could propagate easily, even for relatively small loads, with no damage in the specimen. By taking the slope of the compliance versus crack length relationship, the fibre toughness values can be calculated using the following equation [12],

$$G_{Ic} = \frac{P_c^2}{2h} \frac{\partial C}{\partial a} \quad (4)$$

where  $P_c$  is the critical load associated with each crack length. The thickness  $h$  was assumed to be equal to the thickness of the side-grooved area  $t$ , which was about 0.8mm and the results for the

toughness associated with fibre fracture in the warp direction are shown in Fig. 8.

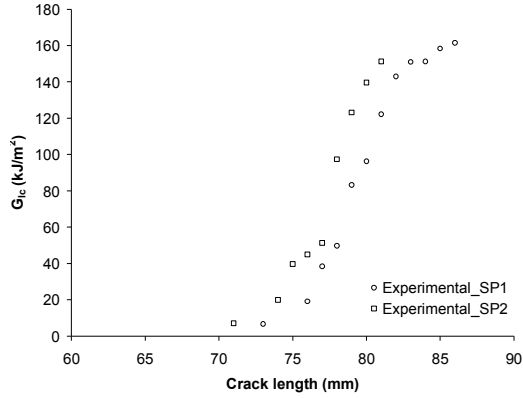


Fig. 8. R-curve for the modified OCT specimens

It is interesting to notice that the low initiation values presented in Fig. 8 are not representative of the carbon fibre toughness but they indicate that some carbon fibres in the cross-sectional area of the side-grooved region were partially damaged during the crack tip preparation stage. This explanation is also confirmed by the sudden increase in toughness from about 50 kJ/m<sup>2</sup> to 100 kJ/m<sup>2</sup> as shown in Fig. 8. This abrupt change indicates that the crack tip has moved from a partially damaged region to an intact region where fibres have no damage and higher energy to create a new crack surface with the same width as the thickness of the side grooved region is required. In light of the facts described above we can conclude that the real toughness associated with crack initiation in the warp direction (carbon fibre direction) is about 100 kJ/m<sup>2</sup> and the propagation values may be about 165 kJ/m<sup>2</sup>. Similar results were reported elsewhere [2,5] using standard OCT specimens and UD pre-preg materials.

## 7 Numerical simulations

### 7.1 Theoretical aspects

The numerical evaluation of the strain energy release rate associated with tensile fibre fracture in the warp direction was based on the J-integral method. For this purpose ABAQUS Standard version 6.5 was used [13]. The software provides a calculation procedure for J-integral based on the virtual crack extension/domain integral methods [13]. Alternatively, the J-integral can be numerically evaluated by measuring the change in strain energy,  $\Delta U$  of the specimen with a crack advance,  $\Delta a$ , where the J-integral is given as the

negative differential of strain energy with respect to crack length that is,

$$J = -\frac{\partial U}{\partial A} \approx \frac{U(a) - U(a + \Delta a)}{h\Delta a} \quad (5)$$

where  $U(a)$  and  $U(a + \Delta a)$  are the strain energies associated with a crack length  $a$  and  $a + \Delta a$ , respectively.  $\Delta a$  is the crack increment and  $h$  is the thickness of the specimen. Although both methods provide the same results in the linear elastic regime, the latter requires extra data post-processing whilst in the former the J-integral values are obtained straightway. For a linear elastic orthotropic material under plane-stress assumption loaded in mode-I opening,  $J = G_{Ic}$  and the stress intensity factor can be related to the J-integral values using [14],

$$K_{Ic}^2 = \frac{J\sqrt{E_{11}E_{22}}}{\sqrt{(\alpha + \beta)/2}} \quad (6)$$

with

$$\alpha = \sqrt{E_{11}/E_{22}} \quad (7)$$

$$\beta = \frac{E_{11}}{2G_{12}} - \nu_{12} \quad (8)$$

### 7.2 FE model for the modified OCT specimen

A three-dimensional orthotropic finite element model including the side-grooved region of the specimen was generated using ABAQUS/Standard to calculate the tensile fibre toughness using the J-integral method. The virtual specimen had dimensions of 115x30x7.2mm<sup>3</sup>. The specimen has a [90/0<sub>3</sub>]<sub>2s</sub> lay-up and each ply was individually modelled using 20-nodes quadratic brick elements. The crack front line was defined along the depth direction by taking the free sides of the elements at the crack tip. The virtual crack extension vector was defined parallel to the crack growth direction. The load was assumed to be uniformly distributed along the loading line of the specimen as shown in Fig. 9.

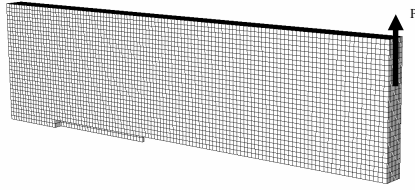


Fig. 9. FE model for the modified CT specimen

Simulations were carried out for each crack length experimentally observed and the J-integral values were evaluated on ten different integral contours. By analysing Eq. (2) it is reasonable to suggest that a possible modification to the standard data reduction scheme is through the finite geometry correction factor, which was originally derived for isotropic materials with standardized dimensions given according to the ASTM E399-90 standard [11]. Assuming that stress/strain fields, geometry and the anisotropy effects are correctly modeled by the finite element method, a new correction function can be derived using the following procedure:

- Compute *J-integral* values for different crack lengths;
- For each  $J_i$  compute function  $F(a)$  which is given by:

$$F(a) = \frac{K_{Ic}^i h \sqrt{w}}{P_i} \quad (9)$$

where  $F(a)$  is the correction function associated with the crack length  $a_i$ ,  $P_i$  is the applied load and  $K_{Ic}^i$  its corresponding stress intensity factor which can be obtained from Eq. (6) and is given by,

$$K_{Ic}^i = \frac{J_i^{0.5} (E_{11} E_{22})^{0.25}}{(\alpha/2 + \beta/2)^{0.25}} \quad (10)$$

- The  $F(a)$  values are plotted against their correspondent crack lengths and the new correction function is obtained by finding the best fit function which interpolates those points.

Fig. 10 compares the values of  $F(a)$  obtained using J-integral method, ASTM standard and the proposed correction function. A linear function with a correlation coefficient of 99.999 % was found to

best fit the numerical results. Thus, the proposed function is given by

$$F(a) = C_1 a - C_2 \quad (11)$$

where the best fit coefficients  $C_1$  and  $C_2$  are 0.1029 and -2.2265, respectively. By comparing the ASTM equation with the proposed one it is possible to see that the ASTM correction function gives completely erroneous results for any range of crack length for the side grooved specimens, as expected. The reasons are because (i) the ASTM equation was originally derived for isotropic materials and (ii) the ASTM correction function is only applicable for certain geometries. Moreover, it was not derived for side-grooved specimens where the stress distribution is completely different from the standard OCT specimen dimensions. A comparison between experimental results obtained using the compliance method, J-integral methods and modified ASTM data reduction scheme is shown in Fig. 11.

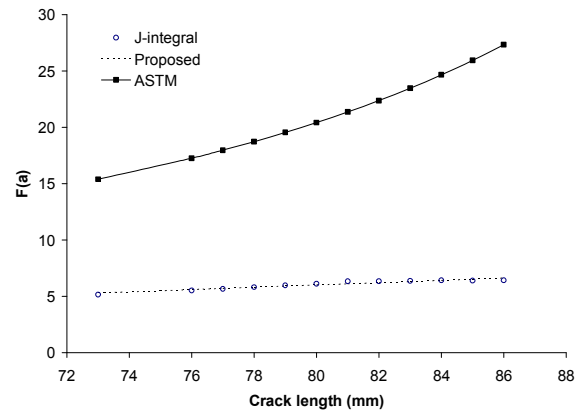


Fig. 10. FE model for the modified CT specimen

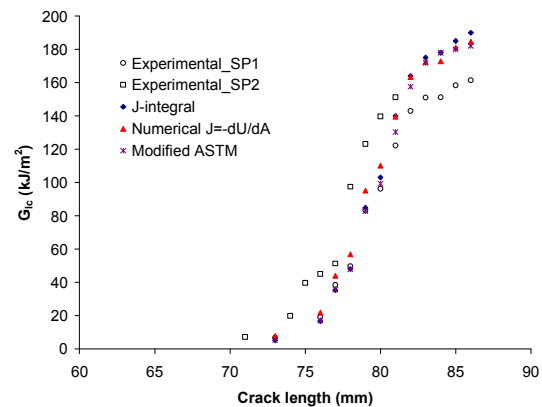


Fig. 11. Comparison between different methods to calculate the tensile fibre fracture toughness

It can be seen from Fig. 11 that the toughness values obtained using the proposed data reduction scheme correlate very well with the toughness values obtained using the compliance and J-integral methods. It also can be noticed that there is an indication that a plateau level may be approached for crack lengths above 85 mm. Various experimental values for fracture initiation could be obtained using the proposed specimen geometry, ranging from a minimum of 7 kJ/m<sup>2</sup> for crack initiation and maximum of 165 kJ/m<sup>2</sup> for crack propagation. In fact, the side-grooved length has to be increased to confirm the propagation values.

## 8. Conclusions

This work presented a detailed numerical and experimental investigation on the intralaminar toughness characterisation of hybrid plain weave laminates under mode I loading using an alternative specimen geometry. Initiation and propagation values around 100 kJ/m<sup>2</sup> and 165 kJ/m<sup>2</sup>, respectively, were obtained for the fibre toughness using the compliance method. It was found that the application of the ASTM E399-90 is fully questionable for composites in general and it can overestimate the toughness values if used in its original form. A methodology to derive a new correction function accounting for geometry and orthotropic effects was presented and discussed in this paper. The methodology can handle different geometries giving better correlation with experimental results compared with standard methods.

## 9. Acknowledgements

The authors acknowledge the financial support received for this work from the Brazilian National Research Council (CNPq), contract number 200863/00-2(NV). The authors are also indebted to Prof. Dr. Sérgio Frascino Muller de Almeida from the Technological Institute of Aeronautics-ITA/Brazil for his discussions and suggestions.

## References

- [1] Cowley D.K., Beaumont P.W.R., "The interlaminar and intralaminar fracture toughness of carbon-fibre/polymer composites: The effect of temperature". *Composite Science and Technology*, Vol. 57, pp. 1433-1444, 1997.
- [2] Konstantinos G.D., Kostopoulos V., Steen M., "Intrinsic parameters in the fracture of carbon/carbon composites". *Composite Science and Technology*, Vol. 65, pp. 883-897, 2005.
- [3] Lin G. Y., Shetty D. "Transformation zones, crack shielding, and crack-growth resistance of Ce-TZP/alumina composite in mode II and combined mode II and mode I loading". *Engineering Fracture Mechanics*, Vol. 70, pp. 2569-2585, 2003.
- [4] Jose S., Kumar R.R., Jana M.K., Rao G.V. Intralaminar fracture toughness of a cross-ply laminate and its constituent sub-laminates". *Composite Science and Technology*; Vol. 61, pp. 1115-1122, 2001.
- [5] Pinho, S.T., Robinson, P., Iannucci L., "Fracture toughness of the tensile and compressive fibre failure modes in laminated composites". *Composite Science and Technology*, Vol. 66, pp. 2069-2079, 2006.
- [6] Kostopoulos V, Markopoulos Y.P., Pappas Y.Z., Peteves S.D. "Fracture energy measurements of 2-D Carbon/Carbon composites". *Journal of European Ceramic Society* Vol.18, pp. 69-79, 1998.
- [7] Donadon M.V., Falzon B.G, Iannucci L., Hodgkinson J.M.. "Intralaminar toughness characterisation of unbalanced hybrid plain weave laminates". *Composites Part A: Applied Science and Manufacturing*, article in press, 2007
- [8] Donadon M.V., Hodgkinson J.M., Falzon B.G., Iannucci L. The reliability of the resin infusion under flexible tooling process for manufacturing composites aerostructures. *In: Proceedings of the 13<sup>th</sup> Sicomp*, Sweden, September, 2004.
- [9] Donadon M.V., Hodgkinson J.M., Falzon B.G., Iannucci L. The impact behaviour of composites manufactured using resin infusion: Mechanical and physical properties assessment, *Internal report*, Dept. of Aeronautics, Imperial College London, 2004.
- [10] Donadon M.V, Hodgkinson J.M., Falzon B.G., Iannucci L. Impact damage in composite structures manufactured using resin infusion under flexible tooling (RIFT) process. *In: Proceedings of the ECCM-11, Greece*, 2004.
- [11] Standard test method for plane strain fracture toughness of metallic materials, ASTM E399-90, *Annual book of ASTM standards* 03.01, pp. 407-528, 1993.
- [12] Slepetz J.M., Carlson L., Fracture of composite compact tension specimens, ASTM STP 593, *American Society for Testing and Materials* 1975.
- [13] ABAQUS 6.5-1., *Theoretical manual*, 2005
- [14] Lin, S. T., Feng Z., Rowlands R.E. Thermoelastic determination of stress intensity factors in orthotropic composites using J-integral. *Engineering Fracture Mechanics*, Vol. 56(4), pp. 579-592, 1997